



Short communication

## Characterization of $\text{Ba}_{1.0}\text{Sr}_{1.0}\text{FeO}_{4+\delta}$ cathode on $\text{La}_{0.9}\text{Sr}_{0.1}\text{Ga}_{0.8}\text{Mg}_{0.2}\text{O}_{3-\delta}$ electrolyte for intermediate temperature solid oxide fuel cells

Yanping Yin<sup>a</sup>, Bangwu Liu<sup>b</sup>, Junjie Qi<sup>b</sup>, Yousong Gu<sup>b</sup>, Qingliang Liao<sup>b</sup>, Zi Qin<sup>b</sup>, Zhanqiang Li<sup>a</sup>, Qinyu Wang<sup>b</sup>, Yue Zhang<sup>a,b,\*</sup>

<sup>a</sup> State Key Laboratory of Advanced Metals and Materials, University of Science and Technology Beijing, Beijing 100083, People's Republic of China

<sup>b</sup> School of Material Science and Engineering, University of Science and Technology Beijing, Beijing 100083, People's Republic of China

## ARTICLE INFO

## Article history:

Received 5 March 2011

Accepted 9 March 2011

Available online 17 March 2011

## Keywords:

Solid oxide fuel cells

Cathode materials

Mixed ionic–electronic conductor

Electrochemical performance

## ABSTRACT

$\text{Ba}_{1.0}\text{Sr}_{1.0}\text{FeO}_{4+\delta}$  (BSFO) with  $\text{A}_2\text{BO}_4$  structure as a cathode material for intermediate temperature solid oxide fuel cells (IT-SOFCs) is synthesized through an ethylene diamine tetraacetic acid (EDTA)–citrate process, and characterized by X-ray diffraction. Field emission scanning electron microscopy shows that BSFO cathode is well attached to the  $\text{La}_{0.9}\text{Sr}_{0.1}\text{Ga}_{0.8}\text{Mg}_{0.2}\text{O}_{3-\delta}$  (LSGM) electrolyte. The electrical conductivity measured by DC four-probe method increases as the temperature increases. A linear relationship between  $\ln(\sigma T)$  and  $1000/T$  indicates that the conducting behavior obeys the small polaron conductivity mechanism. Electrochemical performance of BSFO cathode on LSGM electrolyte is investigated in the temperature range from 500 °C to 800 °C. The results indicate that oxygen adsorption/dissociation process dominates cathodic reaction. Furthermore, the polarization resistance of BSFO cathode decreases with increasing temperature, and declines to  $1.42 \Omega \text{cm}^2$  at 800 °C. These results show that BSFO can be a promising cathode material used on LSGM electrolyte for IT-SOFCs.

© 2011 Elsevier B.V. All rights reserved.

### 1. Introduction

Solid oxide fuel cells (SOFCs) have been considered as one of the most promising energy conversion devices due to their fuel variety, high efficiency and low environmental pollution [1]. Conventional SOFCs have to work at a high temperature (>1000 °C), which not only increase their cost but also reduce their material diversification. Therefore, SOFCs working at intermediate or low temperatures (500–800 °C) are of great interest [2]. However, even with these, performances of these cells usually deteriorate at intermediate operating temperatures, mainly due to internal resistances between electrolytes and cathodes [3]. It is necessary to develop new cathode materials with low polarization resistances at intermediate operating temperatures.

Recently, compounds with  $\text{A}_2\text{BO}_4$  structure have generated considerable interest as cathode materials for intermediate temperature solid oxide fuel cells (IT-SOFCs). The  $\text{A}_2\text{BO}_4$  structure, with a lanthanide at A site and a transition metal cation (Ni, Co, Cu, Fe) at B site, can be considered as both  $\text{ABO}_3$  perovskite structure and

AO rock-salt layers arranging alternatively in the *c*-direction. This structure can produce a lot of interstitial oxygen defects with negative charges, which is beneficial to the transport of oxygen ions [4–8]. In order to produce dramatically improved electrochemical properties, several systems have been either doped or replaced A site with alkaline-earths. Li et al. investigated Sr doped  $\text{La}_2\text{CuO}_4$  as cathode materials for IT-SOFCs with GDC electrolyte, and found that  $\text{La}_{1.7}\text{Sr}_{0.3}\text{CuO}_4$  electrode exhibited optimized performances [5]. Zhao et al. studied the conductivity of  $\text{La}_{2-x}\text{Sr}_x\text{Co}_{0.8}\text{Ni}_{0.2}\text{O}_{4+\delta}$  (LSCN,  $x=0, 0.4, 0.8, 1.2, 1.6$ ) and  $\text{Ce}_{0.9}\text{Gd}_{0.1}\text{O}_{1.95}$  (GDC) composite cathodes, and found that  $\text{La}_{1.2}\text{Sr}_{0.8}\text{Co}_{0.8}\text{Ni}_{0.2}\text{O}_{4+\delta}$ -based electrode had the lowest interfacial polarization resistance ( $1.36 \Omega \text{cm}^2$  at 600 °C) [6]. Jin et al. evaluated the performance of  $\text{Ba}_{2-x}\text{Sr}_x\text{FeO}_{4+\delta}$  ( $x=0.5, 0.6, 0.7, 0.8, 1.0$ ) on a samarium doped ceria (SDC) electrolyte. The best electrochemical properties during the reduction process were observed at  $x=1.0$ . The polarization resistance of  $\text{Ba}_{1.0}\text{Sr}_{1.0}\text{FeO}_{4+\delta}$  on SDC electrolyte was  $1.11 \Omega \text{cm}^2$  at 700 °C [9].

Most of these researches evaluated the electrochemical performance of cathode materials with  $\text{A}_2\text{BO}_4$  structure on doped ceria electrolyte, but little attention was paid to the doped  $\text{LaGaO}_3$  electrolyte. In addition, substitution of the small  $\text{La}^{3+}$  ions by  $\text{Ba}^{2+}$  and  $\text{Sr}^{2+}$  could produce more oxygen overstoichiometry, which resulted in better electrochemical properties. In this study,  $\text{Ba}_{1.0}\text{Sr}_{1.0}\text{FeO}_{4+\delta}$  (BSFO) powders were prepared by EDTA–citrate method. The electrical conductivity and the electro-

\* Corresponding author at: State Key Laboratory of Advanced Metals and Materials, University of Science and Technology Beijing, Beijing 100083, People's Republic of China. Tel.: +86 10 62334725; fax: +86 10 62333113.

E-mail address: [yuezhang@ustb.edu.cn](mailto:yuezhang@ustb.edu.cn) (Y. Zhang).

chemical performance of BSFO cathode on LSGM electrolyte were investigated.

## 2. Experimental

### 2.1. Preparation

Ba<sub>1.0</sub>Sr<sub>1.0</sub>FeO<sub>4+δ</sub> (BSFO) powders were synthesized by a modified citric acid sol-gel method. Stoichiometric amounts of analytical-grade Ba(NO<sub>3</sub>)<sub>2</sub>, Sr(NO<sub>3</sub>)<sub>2</sub>, and Fe(NO<sub>3</sub>)<sub>3</sub>·9H<sub>2</sub>O were dissolved in deionized water. The nitrate solution was mixed with 1 M EDTA-NH<sub>4</sub>OH solution by magnetic stirring and the mixture was heated to 90 °C in a water bath. Then citric acid was added into the mixture, and the mole ratio of the total metal ions:EDTA: citric acid was controlled to approximately 1:1:1.5. To prevent precipitation, NH<sub>4</sub>OH was added to adjust the pH value to about 6. During this process the solution turned into viscous liquids. The viscous liquids were transferred into a beaker which was maintained at 200–250 °C until auto-combustion occurred. The as-synthesized powders were calcined at 800–1100 °C for 8 h in air and BSFO powders were obtained.

### 2.2. Fabrication of symmetrical fuel cells

The synthesis of LSGM powders has been detailed elsewhere [10]. As-prepared LSGM powders were pressed uniaxially into pellets and sintered at 1350 °C for 5 h in air. The samples obtained were about 12 mm in diameter and 0.5 mm in thickness. Cathode slurry was prepared by mixing BSFO powders and ethyl cellulose with a weight ratio of 1:1, and dispersed homogeneously in terpineol in an ultrasonic bath. The slurry was then sprayed onto both sides of LSGM electrolyte. In order to obtain a symmetrical fuel cell, the electrolyte with cathode slurry was calcined at 600 °C for 1 h in air to eliminate organic binders and subsequently sintered at 1000 °C for 3 h. Pt paste was brushed onto both sides of the symmetrical fuel cell to serve as current collectors. Pt leads were connected to the Pt paste to measure the electrochemical properties of the cell.

### 2.3. Characterization

X-ray diffraction (XRD) was carried out on a Rigaku Dmax-RB X-ray diffractometer with Cu K $\alpha$  radiation at a scanning rate of 0.02° per step to identify the phases formed in the cathode. The morphology of the cathode on LSGM electrolyte after sintering was observed by a field emission scanning electron microscope (FESEM, SUPPA-55) with a voltage of 10 kV. In order to measure the electrical conductivity of the cathode, bars were made following a normal calcine-grind-press-sinter process. The electrical conductivity of the sintered bars was measured by DC four-probe equipment from 300 °C to 800 °C in air. Electrochemical impedance spectroscopy (EIS) measurements of the cathode materials on the

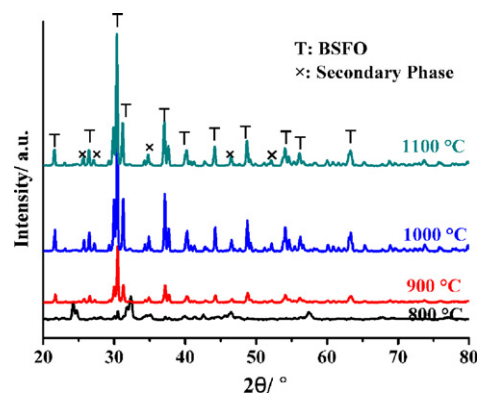


Fig. 1. XRD patterns of BSFO powder calcined at different temperatures.

LSGM electrolyte were carried out from 500 °C to 800 °C in air with a Solartron 1260 Impedance/Gain-Phase Analyzer coupled with Solartron 1287 electrochemical interface. The applied frequency ranged from 10<sup>6</sup> Hz to 10<sup>-2</sup> Hz with a perturbation amplitude of 10 mV.

## 3. Results and discussion

### 3.1. Structure characterization

The XRD spectra of BSFO powders calcined at different temperatures for 8 h are shown in Fig. 1. It is found that A<sub>2</sub>BO<sub>4</sub> structure is not formed when the calcination temperature is below 900 °C. Fig. 2 exhibits the FESEM images of the BSFO cathode on the LSGM electrolyte sintered at 1000 °C for 3 h. Fig. 2(a) demonstrates that the particles are connected with each other, with an average grain size of about 1–2 μm. The cathode provides a well-boned porous network to transport the gas, which facilitates the oxygen reduction reaction. The porous BSFO cathode is attached to the dense LSGM electrolyte, and no cracks are observed at the BSFO/LSGM interface, as illustrated in Fig. 2(b).

### 3.2. Electrical conductivity

In mixed ion-electronic conductor, both ions and electrons would contribute to transport properties. However, since electronic conductivity is usually much higher than ionic conductivity, the total conductivity measured is mainly determined by the electronic conductivity. Fig. 3(a) displays the variation of electrical conductivities with temperatures. As the temperature increases from 300 °C to 800 °C, the electrical conductivities reveal an upward shift. The Arrhenius plot corresponding to Fig. 3(a) is given in Fig. 3(b). The results show the relationship between ln( $\sigma T$ ) and 1000/T is nearly linear, which indicates that the conducting behavior obeys the

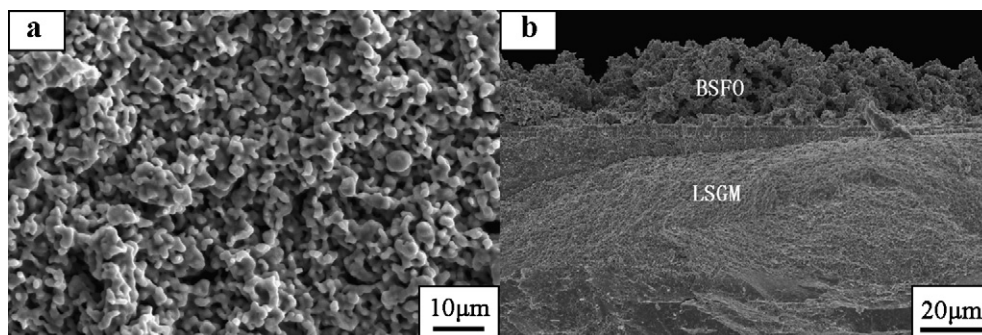


Fig. 2. SEM morphology of BSFO cathode on LSGM electrolyte sintered at 1000 °C (a) surface view and (b) cross-section view.

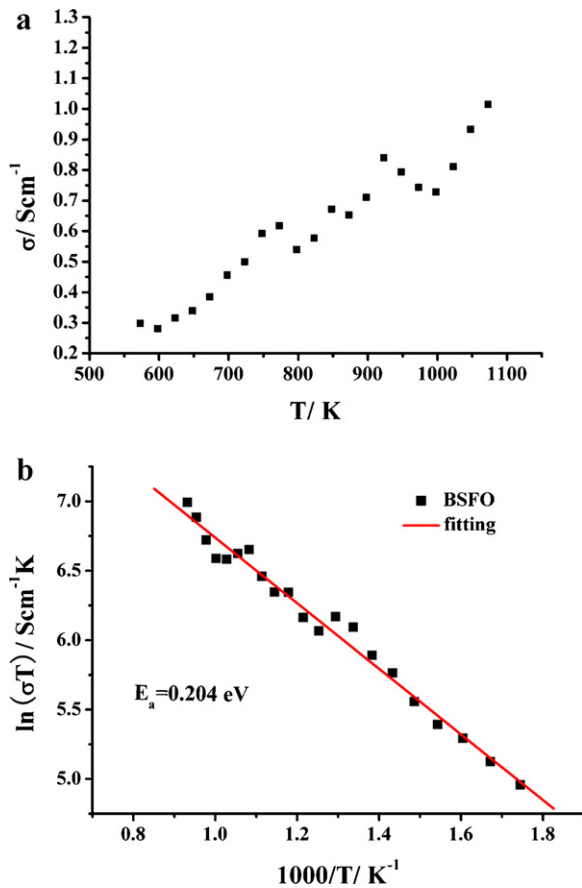


Fig. 3. (a) Electrical conductivity of BSFO specimen measured in air from 300 °C to 800 °C and (b) the corresponding Arrhenius plots.

small polaron conductivity mechanism according to the Arrhenius' equation:

$$\sigma = \left(\frac{A}{T}\right) \exp\left(\frac{-E_a}{kT}\right) \quad (1)$$

where  $A$  is a pre-exponential factor,  $k$  is the Boltzman's constant,  $T$  is the absolute temperature and  $E_a$  is the activation energy. The  $E_a$  calculated from the linear fit is 0.204 eV.

### 3.3. Electrochemical performance

Electrochemical impedance measurements for BSFO cathode on LSGM electrolyte were performed at different temperatures without applying a bias voltage in air, as shown in Fig. 4. The equivalent circuits are also shown in the inset, where  $L$  denotes an inductance,  $R_s$  is the ohmic resistance of the cell,  $Q$  is a constant phase element,  $R_1$  and  $R_2$  are the polarization resistances at high and low frequencies, respectively, and  $R_p$ , the sum of  $R_1$  and  $R_2$ , is the polarization resistance of the cathode/electrolyte interface. The impedance spectra can be fitted by a nonlinear least squares fitting

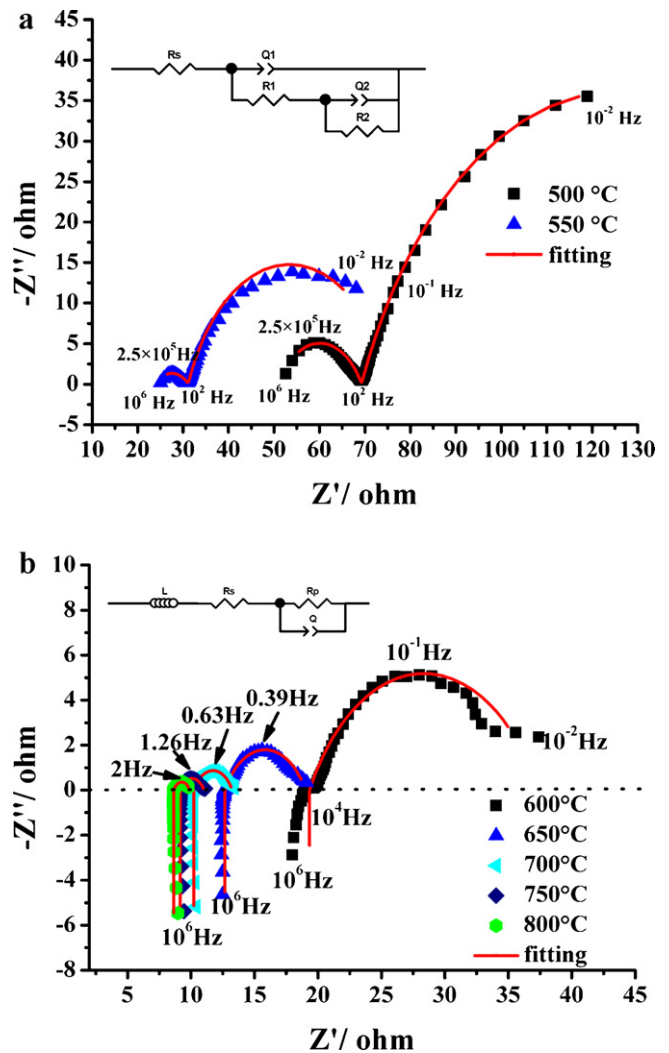


Fig. 4. AC impedance spectra of BSFO cathode on LSGM electrolyte measured in air without bias voltage in the temperatures range of (a) 500–550 °C and (b) 600–800 °C. The equivalent circuits are shown in the inset.

program (ZSimpWin 3.1), and the results obtained are shown in Table 1. From Table 1, the value of  $R_p$  decreases as the temperature increases, and declines to 1.42  $\Omega \text{ cm}^2$  at 800 °C.  $Q$ , a non-ideal capacitor, is similar to a true capacitor ( $C$ ) and can be transformed into  $C$  with the following equation [11]:

$$C_i = (R_i Q_i)^{1/n_i} / R_i \quad (2)$$

In Fig. 4(a), there are two arcs in the impedance spectra measured at 500 °C and 550 °C, which implies that there are two different processes occurring in the cathode reaction. The small arc on the left corresponds to a high frequency process and the large arc on the right corresponds to a low frequency process. The capacitances at high frequencies ( $C_1$ ) are around  $10^{-8} \text{ F cm}^{-2}$ ,

Table 1  
Polarization resistances and capacitances of BSFO cathode on LSGM electrolyte at different temperatures.

$T$ (°C)	$R_1$ ( $\Omega \text{ cm}^2$ )	$C_1$ ( $\text{F cm}^{-2}$ )	$R_2$ ( $\Omega \text{ cm}^2$ )	$C_2$ ( $\text{F cm}^{-2}$ )	$R_p$ ( $\Omega \text{ cm}^2$ )	$C$ ( $\text{F cm}^{-2}$ )
500	20.70	$5.3 \times 10^{-8}$	127.58	0.191	148.28	–
550	8.20	$6.8 \times 10^{-8}$	44.57	0.116	52.77	–
600	–	–	–	–	20.39	0.088
650	–	–	–	–	7.17	0.065
700	–	–	–	–	3.42	0.061
750	–	–	–	–	2.13	0.0608
800	–	–	–	–	1.42	0.060

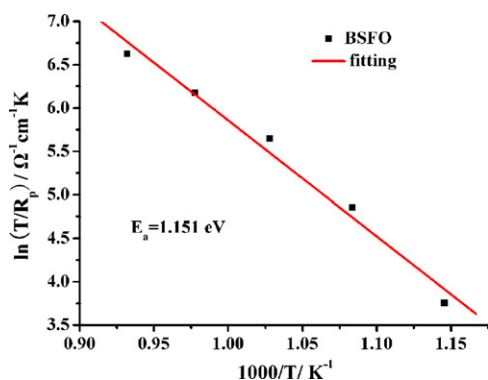


Fig. 5. The Arrhenius plot of the polarization resistance of BSFO cathode on LSGM electrolyte.

which can be ascribed to the process in which the oxygen ions transfer from surface sites to oxygen vacancies of the cathode or to the grain boundaries of the LSGM electrolyte. However, the capacitances at low frequencies ( $C_2$ ) are found to be around  $10^{-1} \text{ F cm}^{-2}$ , which is possibly attributable to the process of oxygen adsorption or dissociation. The arc on the right is bigger than that on the left, which indicates that oxygen adsorption or dissociation process dominates the cathodic reaction. In Fig. 4(b), only one arc appears in the impedance spectra measured from 600 °C to 800 °C. As the temperature increases, the left arc gradually disappears. The corresponding capacitances are in the range of 0.06–0.09  $\text{F cm}^{-2}$ . Furthermore, the activation energy calculated from the Arrhenius plot of the  $\ln(T/R_p)$  versus the  $1000/T$  in Fig. 5 is 1.151 eV. Therefore, this process can be attributed to the dissociation of molecular oxygen and the diffusion of atomic oxygen [12,13].

#### 4. Conclusions

In summary, BSFO powders were prepared by EDTA–citrate method and their electrical conductivities and electrochemical

performances were investigated. X-ray diffraction spectra show that the  $\text{A}_2\text{BO}_4$  structure is obtained for BSFO powders calcined at 900 °C for 8 h. Electrical conductivity increases with increasing temperature and electronic conduction adopts the small polaron mechanism. The impedance spectra show the polarization resistance of the BSFO cathode in air decreases as the temperature increases and declines to  $1.42 \Omega \text{ cm}^2$  at 800 °C, and oxygen adsorption/dissociation dominates cathodic reaction. These results indicate that BSFO holds great potential as a cathode material to be used on LSGM electrolyte for IT-SOFCs.

#### Acknowledgements

This work was supported by the National Basic Research Program of China (No. 2007CB936201), the Major Project of International Cooperation and Exchanges (No. 2006DFB51000), and the Research Fund of Co-construction Program from Beijing Municipal Commission of Education.

#### References

- [1] N.Q. Minh, *J. Am. Ceram. Soc.* 76 (1993) 563–588.
- [2] A. Montenegro Hernández, L. Mogni, A. Caneiro, *Int. J. Hydrogen Energy* 35 (2010) 6031–6036.
- [3] D. Pérez-Coll, A. Aguadero, M.J. Escudero, L. Daza, *J. Power Sources* 192 (2009) 2–13.
- [4] A. Aguadero, J.A. Alonso, M.J. Escudero, L. Daza, *Solid State Ionics* 179 (2008) 393–400.
- [5] Q. Li, H. Zhao, L.H. Huo, L.P. Sun, X.L. Cheng, J.C. Grenier, *Electrochem. Commun.* 9 (2007) 1508–1512.
- [6] F. Zhao, X.F. Wang, Z.Y. Wang, R.R. Peng, C.R. Xia, *Solid State Ionics* 179 (2008) 1450–1453.
- [7] J.B. Huang, R.F. Gao, Z.Q. Mao, J.Y. Feng, *Int. J. Hydrogen Energy* 35 (2010) 2657–2662.
- [8] Y.F. Wang, J.G. Cheng, Q.M. Jiang, J.F. Yang, J.F. Gao, *J. Power Sources* 196 (2011) 3104–3108.
- [9] C. Jin, J. Liu, Y.H. Zhang, J. Sui, W.M. Guo, *J. Power Sources* 182 (2008) 482–488.
- [10] B.W. Liu, L.D. Tang, Y. Zhang, *Int. J. Hydrogen Energy* 34 (2009) 440–445.
- [11] J. Fleig, *Solid State Ionics* 150 (2002) 181–193.
- [12] M.J. Jorgensen, M. Mogensen, *J. Electrochem. Soc.* 148 (2001), 443–442.
- [13] E.V. Tsipis, E.N. Naumovich, A.L. Shaula, M.V. Patrakeev, J.C. Waerenborgh, V.V. Kharton, *Solid State Ionics* 179 (2008) 57–60.